# Failure To Open the Blood-Brain Barrier and Deliver Immune Effectors to Central Nervous System Tissues Leads to the Lethal Outcome of Silver-Haired Bat Rabies Virus Infection[∇]

Anirban Roy, Timothy W. Phares, Hilary Koprowski, and D. Craig Hooper*

*Center for Neurovirology, Kimmel Cancer Center, Thomas Jefferson University,
1020 Locust Street, Philadelphia, Pennsylvania 19107*

**Rabies is a lethal disease caused by neurotropic viruses that are endemic in nature. When exposure to a potentially rabid animal is recognized, prompt administration of virus-neutralizing antibodies, together with active immunization, can prevent development of the disease. However, once the nonspecific clinical symptoms of rabies appear conventional postexposure treatment is unsuccessful. Over the last decade, rabies viruses associated with the silver-haired bat (SHBRV) have emerged as the leading cause of human deaths from rabies in the United States and Canada as a consequence of the fact that exposure to these viruses is often unnoticed. The need to treat SHBRV infection following the development of clinical rabies has lead us to investigate why the immune response to SHBRV fails to protect at a certain stage of infection. We have established that measurements of innate and adaptive immunity are indistinguishable between mice infected with the highly lethal SHBRV and mice infected with an attenuated laboratory rabies virus strain. While a fully functional immune response to SHBRV develops in the periphery of infected animals, the invasion of central nervous system (CNS) tissues by immune cells is reduced and, consequently, the virus is not cleared. Our data indicate that the specific deficit in the SHBRV-infected animal is an inability to enhance blood-brain barrier permeability in the cerebellum and deliver immune effectors to the CNS tissues. Conceivably, at the stage of infection where immune access to the infected CNS tissues is limited, either the provision or the development of antiviral immunity will be ineffective.**

The outcome of a virus infection of the central nervous system (CNS) is dictated by the nature of the cells in which the virus replicates, the extent of virus spread, and the characteristics of the immune response to the infection. A virus may be cleared from CNS tissues with relatively little permanent damage provided that the appropriate immune effectors become active before virus replication is too extensive, particularly if neurons are infected. If inappropriate immune mechanisms are triggered or antiviral immunity develops late in an infection, immunopathology may make a significant contribution to disease. On the other hand, in the absence of immune recognition, pathogenicity directly caused by the virus is the determining feature of the infection.

The etiological agents of the lethal neurological disease rabies, rabies virus (RV) strains, are found extensively in nature, each associated with a particular host species (17). In the United States and Canada, an RV strain associated with the silver-haired bat (SHBRV) is the major cause of human deaths from rabies (4, 18). The elusive mode of infection with this virus, together with the lack of specific signs and symptoms of rabies, makes the diagnosis and treatment of SHBRV infection extremely difficult (1, 2).

The contribution of immunity toward controlling a pathogenic RV infection is highlighted by the fact that a combination of active and passive immunization, termed rabies postexposure prophylaxis (PEP), within the first days after exposure to a pathogenic variant is the only known means of preventing the development of the disease in humans (27). The fact that postexposure immunization is necessary to prevent the onset of clinical rabies in humans provides evidence that the immune response to the natural infection develops either too slowly, inappropriately, or not at all. While PEP is highly effective when administered soon after infection, it provides little benefit once clinical signs of rabies appear (3). One school of thought is that RV becomes sequestered from the immune system when it reaches the CNS (25). However, studies of laboratory-adapted RV strains antigenically related to SHBRV but with little to no pathogenicity for immunocompetent animals have revealed that RV can be cleared from infected CNS tissue (13). For example, CVS-F3, a less pathogenic variant of challenge virus standard (CVS), spreads to the CNS tissues of mice from peripheral sites of inoculation but nevertheless induces an immune response that clears the virus without sequelae (21). In addition to antigen-specific antiviral immunity, an innate response of CNS-resident cells to the virus, together with enhanced blood-brain barrier (BBB) permeability, is likely to contribute to the CNS inflammatory response that has been associated with clearance of CVS-F3 from CNS tissues (21). In contrast to mice infected with CVS-F3, CNS inflammation is rarely seen in humans dying from infection with pathogenic strains of RV (20). Moreover, when SHBRV strains isolated from human victims of the disease are used to infect mice, a similar pattern of lethality with limited inflammatory changes in CNS tissues is seen (28). This suggests that

* Corresponding author. Mailing address: Center for Neurovirology, Thomas Jefferson University, 1020 Locust St., JAH 454, Philadelphia, PA 19107-6799. Phone: (215) 503-1774. Fax: (215) 923-7745. E-mail: douglas.hooper@jefferson.edu.

some aspect of the immune response to SHBRV may be deficient. To determine whether this is the case, we have compared the development of innate and adaptive immune responses in the periphery and CNS of mice infected with an SHBRV variant and mice infected with CVS-F3.

## MATERIALS AND METHODS

**Animals and virus infection.** $rag-2^{-/-}$ mice, which are deficient in T and B cells, as well as congenic control 129/SvEv mice, were purchased from Taconic Farms and used at 8 to 10 weeks of age. Mice were infected with either CVS-F3 RV, an antibody escape-attenuated mutant differing from its parental CVS strain at a single amino acid, Arg→Glu-333 (11), or SHBRV-17, a pathogenic strain originally isolated from human brain tissue and expanded via several passages in neonatal mouse brain (9). Immunocompetent wild-type mice were infected intradermally (i.d.) in both ears with $10^5$ focus-forming units (FFU) of CVS-F3 or $10^4$ FFU (10 i.d. 50% lethal doses) of SHBRV-17 in 10 μl of phosphate-buffered saline (PBS). In reconstitution experiments, $rag-2^{-/-}$ mice were infected via the intranasal route with $10^5$ FFU of CVS-F3 in 10 μl of PBS because this rapidly delivers virus to the CNS in the absence of a proinflammatory needle stick. All procedures, including housing of mice, were carried out according to protocols approved by the Institutional Animal Care and Use Committee of Thomas Jefferson University.

**Quantitative RT-PCR.** Expression levels of different genes were measured by quantitative real-time PCR (RT-PCR) as previously described (21). Briefly, total RNA was isolated from the CNS tissues of RV-infected and uninfected control mice with a QIAGEN RNeasy kit. cDNAs were synthesized from mRNA by reverse transcription with oligo(dT) as the primer. RT-PCR was then performed with TaqMan PCR reagents, gene-specific primers and probes, synthetic gene standards, and a Bio-Rad iCycler iQ Real Time Detection System. The mRNA copy numbers of a particular gene in each sample were normalized to the mRNA copy number of a housekeeping gene (L13) in that sample. To estimate virus replication, virus-specific nucleoprotein mRNA expression was measured by quantitative RT-PCR and expressed as the number of mRNA copies per milligram of tissue. This has been demonstrated to be a reliable measurement of RV replication (14). The sequences of the primers and probes used for quantitative PCR have been previously detailed (21), with the exception of those for SHBRV-17 nucleoprotein mRNA detection, which were as follows: forward primer, 5′-TGTGCGCTAACTGGAGTACCA-3′; reverse primer, 5′-GTGCCTACCCTAATTGCTGAA-3′; probe, 5′-CCGAACTTCAGATTC CTAGCTGGAACC-3′.

**Measurement of serum antibody titers.** Levels of RV-specific total immunoglobulin G (IgG) and the IgG1 and IgG2a isotypes in sera from mice infected with CVS-F3 or SHBRV-17, as well as uninfected controls, were assessed by enzyme-linked immunosorbent assay (ELISA) as described previously (6). Briefly, 96-well plates (Nalge Nunc International) were coated with UV-inactivated RV and antibodies captured from serially diluted samples of sera were detected with peroxidase-conjugated anti-mouse IgG (Sigma) or alkaline phosphatase-conjugated anti-mouse IgG1 (Pharmingen) or IgG2a (Cappel) and the appropriate substrate. Absorbance was measured at 450 nm for peroxidase activity and at 405 nm for phosphatase activity in a microplate spectrophotometer (Biotek). Virus-neutralizing antibody (VNA) titers in the serum samples were determined by the rapid fluorescent focus inhibition test as previously described (12). Briefly, serially diluted serum samples were incubated with CVS-11 and then the mixture was added to baby hamster kidney cells. After 18 h of incubation, cells were fixed and stained with a fluorescein isothiocyanate (FITC)-conjugated anti-RV nucleoprotein antibody and FFU were counted. The VNA titer was determined as the last dilution of serum that was capable of reducing the number of FFU by 50%.

**Immunohistochemistry.** Brains from uninfected and CVS-F3- or SHBRV-17-infected mice were snap-frozen in Tissue-Tek OCT Compound (Sakura Fintex) and cut into 10-μm-thick sections with a Thermo Shandon cryostat as previously described (21). To detect virus-infected cells, cerebellar sections were stained with FITC-conjugated anti-RV nucleoprotein monoclonal antibodies (Centocor). To detect immune cell infiltration in the cerebellum and intracellular adhesion molecule 1 (ICAM-1) expression on neurovasculature, sections were stained with phycoerythrin-conjugated anti-mouse CD4 and FITC-conjugated anti-mouse ICAM-1 antibodies (BD Pharmingen). Photographs were taken with a Nikon Coolpix 995 digital camera attached to a Leitz Microlab microscope and are presented at a final magnification of ×200.

**Flow cytometry.** Erythrocyte-depleted cells collected from the spleen and peripheral blood were washed in PBS and stained with monoclonal antibodies against the mouse pan-T-cell marker CD3, as well as the subset markers CD4 and CD8 (BD Pharmingen). Antibody-labeled cells were washed and fixed in PBS with 0.37% formaldehyde. To identify cells expressing gamma interferon (IFN-γ), the cells were then incubated overnight with permeabilization buffer (0.5% saponin, 0.005% Tween 20, 0.2% fetal bovine serum, and 0.1% NaN$_3$ in PBS), stained with anti-mouse IFN-γ monoclonal antibody (BD Pharmingen), washed in PBS, and resuspended in PBS-formaldehyde. Phenotypic characterization of antibody-labeled cells was performed on a BD FACScalibur flow cytometer.

**Assessment of BBB integrity.** BBB integrity was assessed by quantifying the leakage of a low-molecular-weight fluorescent marker (Na-fluorescein; molecular weight, 376) from the circulation into CNS tissues as previously described (21). Briefly, 100 μl of a 10% solution of Na-fluorescein was injected intraperitoneally and after 10 min mice were anesthetized and cardiac blood was collected, followed by transcardial perfusion with PBS. Supernatants of homogenized and centrifuged tissues, as well as from serum samples, were clarified by precipitating proteins with 15% trichloroacetic acid, and the level of fluorescence was measured with a CytoFluorII fluorimeter. The amount of Na-fluorescein in the CNS tissue is normalized to its level in serum as follows: (micrograms of Na-fluorescein in CNS tissue/milligram of tissue)/(micrograms of Na-fluorescein in serum/microliter of serum).

**Adoptive transfer of immune cells.** Spleens and inguinal, axillary, and cervical lymph nodes were collected from donor mice 6 days after infection. Single-cell suspensions were prepared by teasing the tissues through a 100G stainless steel wire mesh into PBS. Erythrocytes were lysed by hypotonic shock, and the cells were washed by centrifugation in PBS as previously described (16). Twenty million cells were injected in 200 μl of PBS either intraperitoneally into immunocompetent recipient mice or into the tail veins of $rag-2^{-/-}$ recipient mice.

**Statistical analyses.** Results are expressed as the mean ± the standard error of the mean. The statistical significance of the differences in gene expression between control and infected groups was tested by the Mann-Whitney test, while differences between serum antibody levels determined by ELISA were assessed by the paired $t$ test.

## RESULTS

**Infections with SHBRV-17 and CVS-F3 RVs have different outcomes.** Groups of 129SvEv mice were infected with either SHBRV-17 or CVS-F3 intradermally in the ear and monitored for survival. The dose of SHBRV-17 used was $10^4$ FFU, while a 10-fold higher dose ($10^5$ FFU) was chosen for the more slowly replicating CVS-F3 strain, such that virus titers in the cerebellum would be equivalent at day 6 postinfection (p.i.). The developing antiviral immune response should be capable of clearing this amount of virus, as CVS-F3 nucleoprotein mRNA levels begin to drop after this point (Fig. 1A). Nevertheless, nucleoprotein mRNA levels continue to rise in SHBRV-17-infected mice (Fig. 1A), with death occurring between 8 and 9 days p.i. while all of the CVS-F3-infected mice survived without showing any overt sign of infection (Fig. 1B). Despite the different outcomes, by using immunohistochemistry for RV nucleoprotein we were unable to detect any difference in the patterns of cells infected with the different RVs (Fig. 1C).

**Equivalent proinflammatory responses are triggered in the CNS tissues of mice infected with SHBRV-17 and CVS-F3.** The expression of proinflammatory cytokines, chemokines, and adhesion molecules in the CNS is a direct consequence of virus replication in the tissue. These molecules greatly contribute to the development of innate immunity against the infection, as well as promote the infiltration of immune and inflammatory cells from the circulation into the CNS tissues. In CVS-F3-infected mice, the upregulation of tumor necrosis factor alpha (TNF-α), ICAM-1, and chemokines such as regulated on activation, normal T expressed and secreted (RANTES), IFN-inducible protein 10 (IP-10), and monocyte chemoattractant protein 1 (MCP-1) precedes the invasion of CNS tissues by
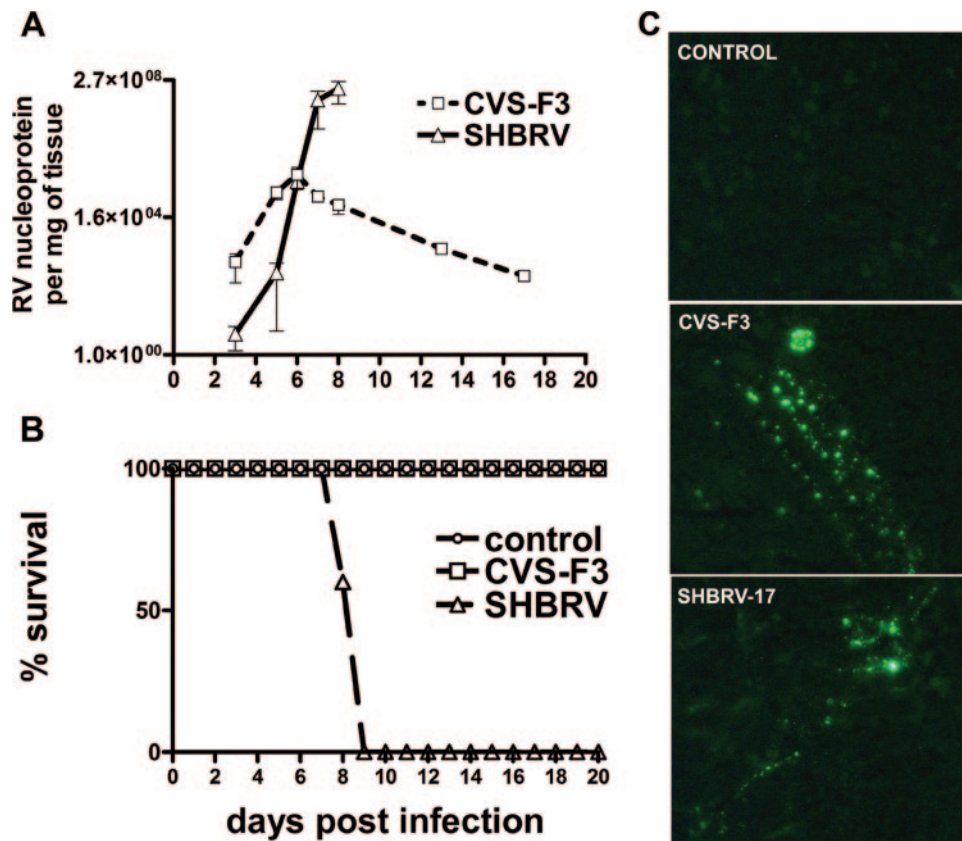
FIG. 1. Comparison of the replication of pathogenic SHBRV-17 and attenuated CVS-F3 RV variants in CNS tissues. Groups of 129 SvEv mice ($n = 5$) were infected with CVS-F3 or SHBRV-17 and either euthanized at the indicated time points to assess RV nucleoprotein mRNA levels in the cerebellum as a measurement of virus replication (A) or monitored for morbidity and mortality (B). Infection and mRNA analysis by quantitative RT-PCR were performed as described in Materials and Methods. Virus-infected cells in frozen cerebellum sections from control and infected mice were identified by immunohistochemistry with FITC–anti-rabies monoclonal antibody (C). Tissue preparation and staining were performed as described in Materials and Methods.

lymphocytes and monocytes (21). A reduction in this innate response to an SHBRV variant has been suggested to be related to its pathogenicity (24). We therefore compared proinflammatory gene expression in CNS tissues from mice 8 days p.i. with SHBRV-17 versus CVS-F3. At this stage of the infection, where the CNS immune and inflammatory response to CVS-F3 becomes significant (21), levels of mRNAs specific for TNF-α, ICAM-1, RANTES, IP-10, and MCP-1 are strongly up-regulated to similar extents in the cerebellum of both SHBRV-17- and CVS-F3-infected mice (Fig. 2A). Similar results were obtained for other regions of the CNS as well (data not shown). Because expression of the adhesion molecule ICAM-1 on neurovasculature plays an important role in CNS inflammation (8), we used immunohistochemistry to confirm the implications of mRNA analysis that ICAM-1 expression is indeed elevated at the protein level on the brain capillary endothelial cells in SHBRV-17-infected mice (Fig. 2B).

**Similar RV-specific antibody responses are elicited by infection with SHBRV-17 versus CVS-F3.** Between days 6 and 8 p.i., virus nucleoprotein mRNA levels decreased in CVS-F3-infected mice but continued to rise in SHBRV-17-infected animals (Fig. 1A). Conceivably, this was because a virus-specific response develops in CVS-F3-infected animals but not in SHBRV-17-infected animals. To determine whether this was

the case, we examined virus-specific antibody levels in sera from both groups of mice. As shown in Fig. 3A, serum RV-specific total IgG titers were somewhat higher in SHBRV-17-infected mice than in CVS-F3-infected mice at 8 days p.i. The serum antibodies were largely of the IgG2a isotype, indicating a bias toward a type 1 response in both infections (Fig. 3B). VNA titers, considered to be of primary importance in a protective RV-specific response (10), were found to be comparable in the sera of mice infected with either virus (Fig. 3C).

**Equivalent cell-mediated response is generated following infection with SHBRV-17 and CVS-F3.** Comparable Th1 humoral responses between CVS-F3- and SHBRV-17-infected mice suggest that T-cell reactivity is likely to be comparable in animals infected with either virus. No significant differences were seen in the distribution of CD4 and CD8 T cells in the two groups of mice at 6 days p.i. (Table 1). However, an elevation in the levels of circulating IFN-γ-positive CD4 T cells was detected in SHBRV-17-infected animals.

**The CNS inflammatory response and enhanced BBB permeability are absent in mice infected with SHBRV-17.** The lethality of infection with SHBRV-17 despite the development of CNS proinflammatory and peripheral virus-specific responses that are comparable to those of apathogenic CVS-F3 infection led us to speculate that the accumulation of immune
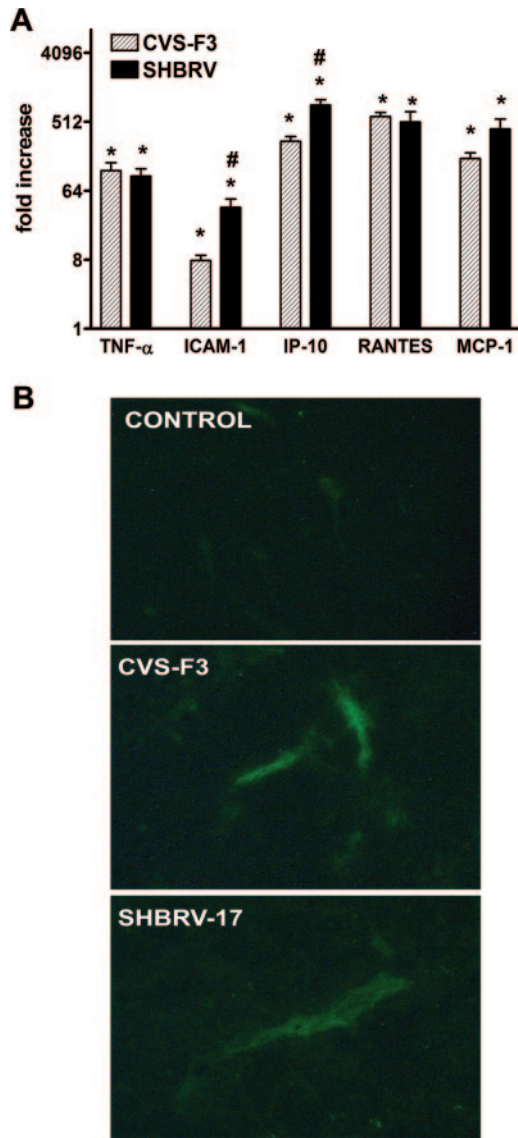
FIG. 2. Proinflammatory responses in the CNS tissues of mice infected with SHBRV-17 and CVS-F3. (A) Levels of mRNAs specific for TNF-$\alpha$, ICAM-1, IP-10, RANTES, and MCP-1 in the cerebellums of groups of six mice either left uninfected or infected with CVS-F3 or SHBRV-17 8 days previously were measured by quantitative RT-PCR as detailed in Materials and Methods. The results are expressed as fold increases in mRNA levels in infected versus uninfected mice. Statistically significant differences determined by the Mann-Whitney test between infected versus uninfected mice and between CVS-F3- versus SHBRV-17-infected mice are denoted by the symbols $*$ ($P < 0.001$) and # ($P < 0.05$), respectively. (B) ICAM-1 expression in the CNS tissues of mice infected with SHBRV-17 and CVS-F3. Sections from the cerebellums of uninfected and CVS-F3- or SHBRV-17-infected mice were prepared and stained with FITC-conjugated anti-mouse ICAM-1 antibody as described in Materials and Methods. Photomicrographs are presented at a final magnification of ×200.
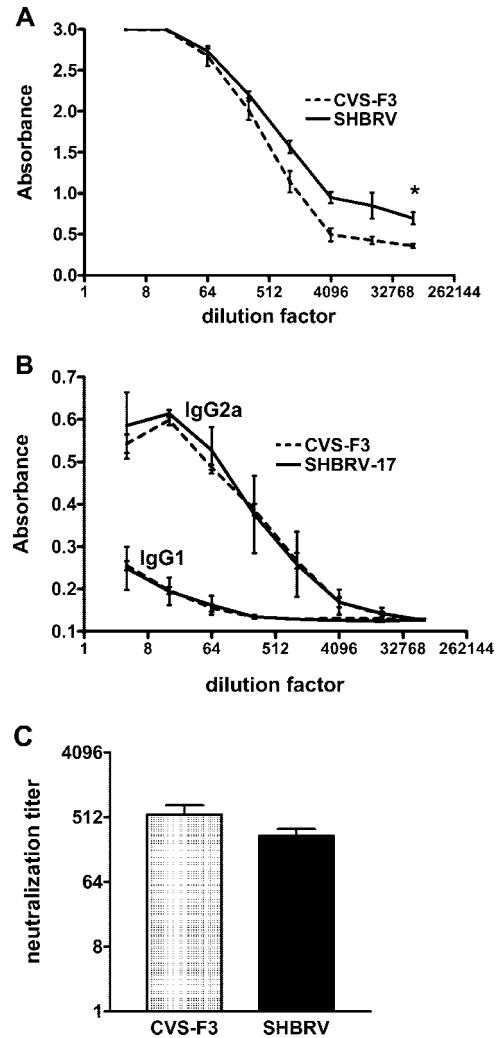


FIG. 3. RV-specific antibody responses elicited by infection with SHBRV-17 versus CVS-F3. Levels of RV-specific total IgG (A), the IgG1 and IgG2a isotypes (B), and VNA (C) in the sera of CVS-F3- and SHBRV-17-infected mice on day 8 p.i. were assessed by ELISA and rapid fluorescent focus inhibition test, respectively, as described in Materials and Methods. Statistically significant differences between groups, calculated by the paired $t$ test, are denoted by asterisks ($P < 0.01$, $n = 10$).

effectors to the CNS tissues may differ between these two infections. Immune cell infiltration of the cerebellum was assessed at day 8 p.i. by determining the levels of mRNAs specific for CD4 and CD8 (T cells) and CD11b (macrophages), as well as CD19 and $\kappa$ light chain (B cells) (Fig. 4A). The levels of all

of these markers were strongly elevated in the cerebellum of CVS-F3-infected mice. In contrast, CD4, CD8, and CD11b mRNA levels were enhanced to a significantly lower extent in the cerebellum of SHBRV-17-infected mice while there was no detectable increase in CD19 and $\kappa$ light chain mRNAs. Immunohistochemical analysis also revealed accumulations of CD4-positive cells in sections from the cerebellum of CVS-F3-infected mice, whereas only a few scattered cells were detected in similar sections from SHBRV-17-infected animals (Fig. 4B). Since BBB permeability changes in the cerebellum are associated with the clearance of CVS-F3 from the CNS (21), we next determined if the deficit in immune cell accumulation in SHBRV-17 infection is associated with a reduction in cerebellar BBB permeability. This proved to be the case (Fig. 4C).

TABLE 1. Different subsets of cell-mediated immunity detected by flow cytometry[a]

| Phenotype[b] | Cell type[c] | Splenocytes | | | PBL[d] | | |
|---|---|---|---|---|---|---|---|
| | | Control | CVS-F3 | SHBRV | Control | CVS-F3 | SHBRV |
| CD3^{+} CD4^{+} | CD4 T cells | 71.96 | 70.82 | 71.93 | 78.59 | 79.31 | 79.05 |
| CD3^{+} CD8^{+} | CD8 T cells | 18.96 | 19.63 | 19.33 | 17.16 | 16.26 | 14.15 |
| CD3^{+} CD8^{−} IFN-γ^{+} | IFN-γ^{+} CD4 T cells | 5.49 | 6.4 | 7.77 | 1.92 | 2.28 | 4.49 |
| CD3^{+} CD8^{+} IFN-γ^{+} | IFN-γ^{+} CD8 T cells | 4.72 | 5.23 | 6.55 | 1.66 | 2.03 | 2.12 |
| CD3^{−} IFN-γ^{+} | IFN-γ^{+} NK cells | 7.07 | 8.98 | 9.93 | 2.35 | 2.62 | 4.1 |

[a] The values shown are percentages of cells gated on the CD3^{+} population, except CD3^{−} IFN-γ^{+} cells, which are presented as percentages of the total number of cells. Data are representative of three independent experiments.
[b] Cells were stained with monoclonal antibodies against mouse surface antigens and IFN-γ as described in Materials and Methods.
[c] Cell types that constitute the major cell populations bearing particular phenotypes.
[d] PBL, peripheral blood lymphocytes.

**Immune cells from mice lethally infected with SHBRV-17 are capable of clearing CVS-F3 from the CNS tissues of *rag-2*^{−/−} mice.** The presence of a peripheral antiviral immune response in SHBRV-17-infected mice that is equivalent to that of CVS-F3-infected animals but reduced cell invasion of the CNS tissues suggests that there may be a defect in the ability of

cells from SHBRV-17-infected animals to enter CNS tissues. To examine this possibility further, we examined whether or not spleen and lymph node cells from SHBRV-17-infected mice can trigger BBB permeability changes, infiltrate the CNS tissues, and clear CVS-F3 from infected *rag-2*^{−/−} mice. CVS-F3-infected *rag-2*^{−/−} mice showed a rapid loss of body
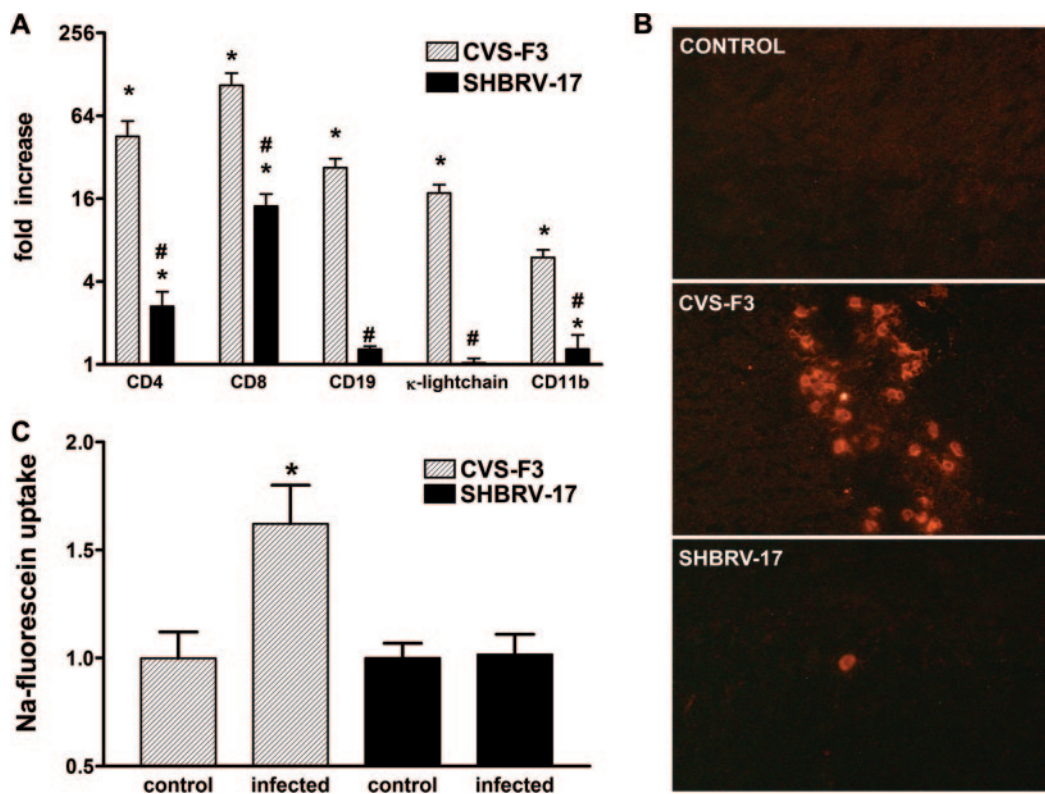


FIG. 4. Immune cell accumulation in the CNS tissues and BBB permeability in mice infected with SHBRV-17 versus CVS-F3. (A) Levels of mRNAs specific for CD4, CD8, CD19, κ light chain, and CD11b in the cerebellum of the CVS-F3-infected, SHBRV-17-infected, and uninfected mice described in the legend to Fig. 2 were measured by quantitative RT-PCR as detailed in Materials and Methods. The results are expressed as fold increases in mRNA levels in infected versus uninfected mice. Statistically significant differences determined by the Mann-Whitney test between infected versus uninfected mice and between CVS-F3- versus SHBRV-17-infected mice are denoted by the symbols ∗ ($P < 0.001$) and # ($P < 0.05$), respectively. (B) Accumulation of CD4-positive cells in the cerebellum of uninfected and CVS-F3- or SHBRV-17-infected mice were identified by immunohistochemistry with phycoerythrin-conjugated anti-mouse CD4 monoclonal antibody as described in Materials and Methods. Photomicrographs are presented at a final magnification of ×200. (C) BBB permeability in the cerebellum was assessed by measuring Na-fluorescein leakage from the circulation into CNS tissues 8 days following infection with CVS-F3 and SHBRV-17 as described in Materials and Methods. The data are expressed as fold increases in Na-fluorescein content over background values obtained with tissues from similarly treated uninfected mice. Statistically significant differences between the groups determined by the Mann-Whitney test are denoted by asterisks ($P < 0.05$, $n = 6$).
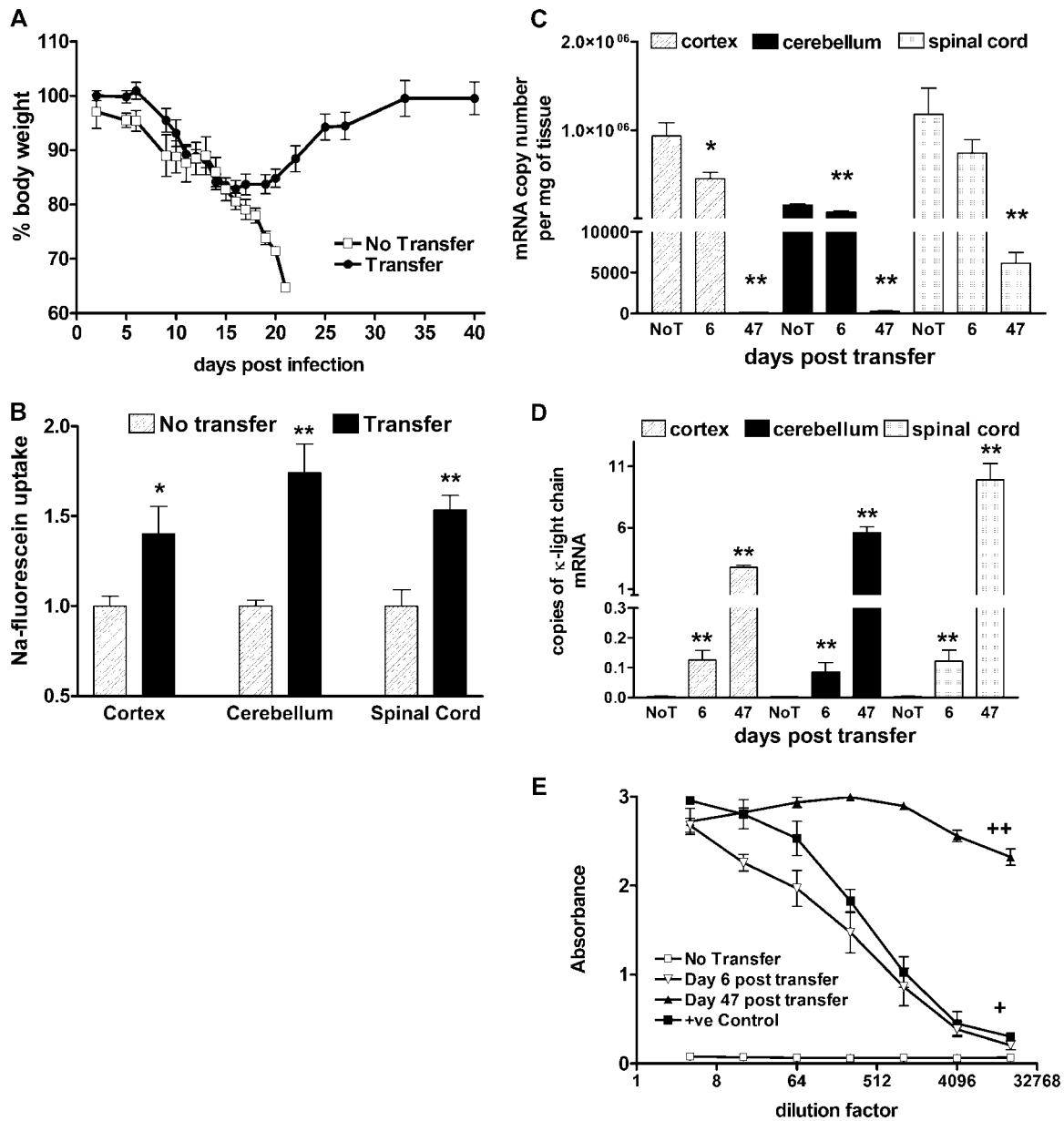
FIG. 5. Effect of adoptive transfer of immune cells from SHBRV-17-infected mice on CVS-F3 infection in $rag$-$2^{-/-}$ mice. $rag$-$2^{-/-}$ mice infected 7 days previously with CVS-F3 were either left unreconstituted (No Transfer, $n = 10$) or received spleen and lymph node cells from congenic mice infected with SHBRV-17 6 days before (Transfer, $n = 10$). The mice were monitored daily for weight and death (A), and BBB permeability changes were assessed in five mice from each group 6 days following transfer (B). Viral nucleoprotein (C) and κ light chain mRNA (D) levels in CNS tissues, as well as serum virus-specific antibody levels (E), were assessed in the no-transfer (No T) and transfer groups on days 6 and 47 following transfer as described in Materials and Methods. Statistically significant differences between the transfer and no-transfer groups in BBB permeability, RV nucleoprotein, and κ light chain mRNA expression determined by the Mann-Whitney test are denoted by asterisks ($P < 0.05$) and double asterisks ($P < 0.001$). Serum antibody levels between these groups were also significantly different as calculated by the paired $t$ test ($+$, $P < 0.01$; $++$, $P < 0.0001$).

weight and, in the absence of cell transfer, succumbed to CVS-F3 infection within 3 weeks of infection (Fig. 5A). However, if spleen and lymph node cells from congenic mice infected with SHBRV-17 6 days previously were transferred to CVS-F3-infected $rag$-$2^{-/-}$ mice, the recipients recovered (Fig. 5A). Six days following cell transfer, BBB permeability was significantly enhanced by comparison with that of CVS-F3-infected $rag$-$2^{-/-}$ mice that did not receive cells (Fig.

5B). The virus load in CNS tissues, as determined by nucleoprotein mRNA levels, was significantly reduced in the recipient mice by day 6 posttransfer, with only trace amounts of nucleoprotein mRNA detected 41 days later (Fig. 5C). κ light chain expression (Fig. 5D), a measurement of B-cell accumulation in CNS tissues, and serum virus-specific antibody titers (Fig. 5E) also increased in the recipient mice over this time frame.
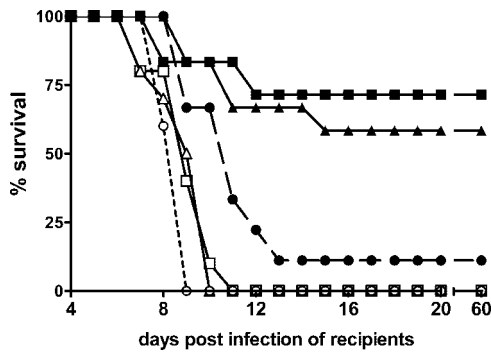
FIG. 6. Effect of adoptive transfer of RV-immune cells on lethal SHBRV-17 infection. Spleen and lymph node cells were adoptively transferred from naive (circles), CVS-F3-infected (triangles), or SHBRV-17-infected (squares) mice to congenic immunocompetent recipient mice either 2 h following (open symbols) or 3 days prior to (filled symbols) infection with SHBRV-17. Recipient mice were monitored daily for clinical signs of rabies and death.

**Adoptive transfer of presensitized immune cells protects recipients against a subsequent challenge with a lethal dose of SHBRV-17 but does not promote clearance of an existing infection.** Even if an antiviral response develops too late in SHBRV-17-infected mice to contain the infection, we expect that the BBB should become permeable and immune effector cells reach the cerebellum in addition to the spinal cord prior to the demise of the animal. Since this is not the case, we speculate that the failure to survive infection with SHBRV-17 is the consequence of some attribute of the virus infection manifested in the loss of the ability to open the BBB in the cortex and cerebellum as opposed to a general deficit in immunity. If so, at some point in the virus infection provision of immune effectors should fail to protect. To test this hypothesis, spleen and lymph node cells obtained from mice 6 days after infection with SHBRV-17 or CVS-F3 were transferred into congenic mice either on the day of or 3 days prior to infection with SHBRV-17. Regardless of whether the donor cells came from SHBRV-17- or CVS-F3-infected animals, transfer prior to a challenge with SHBRV-17 protected the majority of the recipients from lethal infection (Fig. 6), possibly by preventing the spread of virus to the CNS tissues. However, when the same cell populations were transferred into recipients 2 h after infection with SHBRV-17, the mice still died within 11 days (Fig. 6). Thus, despite sensitization to viral antigens in the donor mice 6 days prior that rendered the cells able to clear an established CNS infection with CVS-F3, they could not contain a developing SHBRV-17 infection. We speculate that this is because SHBRV-17 had sufficient time to spread to the CNS and activate the processes inhibiting immune cell invasion before the transferred cells could protect.

## DISCUSSION

Neurotropic viruses that are antigenically related but differ in pathogenicity, as well as the ability to induce a protective immune response during an infection, provide unique tools to probe the relationship between viral neuropathogenicity and immunogenicity. RVs, which exist as a range of antigenically related variants that are highly diverse in pathogenicity, are

particularly useful for such studies. CVS-F3, an RV variant attenuated by a single amino acid substitution in the glycoprotein of CVS (11), is cleared from the CNS of infected, immunocompetent mice as BBB permeability becomes enhanced and immune effectors accumulate in the infected tissues (21). Although CVS-F3 spreads extensively through the cortex and cerebellum, BBB permeability changes, as well as CD4 and B-cell infiltration, are considerably higher in the cerebellum, suggesting that the delivery of antiviral effectors is predominantly through the BBB of the cerebellum (21). This is supported by the present findings that mice infected with SHBRV-17, a pathogenic RV obtained from a human victim of rabies, while developing strong virus-specific immunity in the periphery, fail to develop increased BBB permeability in the cerebellum with its associated CNS inflammatory response and succumb to rabies. Notably, CNS inflammation is seldom seen in animals infected with pathogenic strains of RV, including other SHBRV variants (19, 28), as well as in postmortem studies of human rabies victims (20). Since the development of RV-specific immunity in the periphery of CVS-F3- and SHBRV-17-infected mice is comparable, the reduced CNS inflammatory response to RV seen in the latter evidently does not result from a major deficit in immunity. It is possible that IFN-γ-positive cells accumulate to higher levels in the circulation of SHBRV-17-infected animals because of a diminished ability to infiltrate CNS tissues. Mechanisms whereby an RV-specific immune response may develop but immune effectors fail to infiltrate CNS tissues include (i) defects in the proinflammatory response of CNS-resident cells (24) and (ii) functional changes at the BBB that permit immune cell invasion.

The invasion of infected CNS tissues by immune effector cells from the circulation is dependent upon a sequence of events that includes the production of proinflammatory cytokines and chemokines by CNS-resident cells. These not only attract cells into the tissues but also induce the expression of the adhesion molecules that allow circulating cells to interact with the cells of the BBB. Thus, a reduction in the proinflammatory response may lead to a failure to induce BBB permeability changes and a protective CNS inflammatory response. A recent study has suggested that strains of RV may differ in the ability to induce a CNS proinflammatory response (24). We expect that the magnitude and kinetics of the innate response to different RV isolates depend upon the ability to spread into and replicate in CNS tissues, as well as, at later stages, to induce immune clearance versus cause disease. Wang et al. found that mRNAs specific for MCP-1, IP-10, RANTES, and a variety of other chemokines and cytokines were strongly elevated in severely paralyzed mice infected with an undisclosed SHBRV isolate but to lesser extents than in similarly afflicted mice infected with the less pathogenic CVS-B2c strain (24). On the basis of the timing of the development of immunity in CVS-F3-infected mice (21) and differences in the spread and replication of SHBRV-17 versus CVS-F3, we adjusted our virus inoculums to cause similar virus loads in the CNS tissues as the innate response develops and performed our comparative analyses at day 8 p.i., when the SHBRV-17-infected mice were still healthy. In our comparison of the upregulation of mRNAs specific for proinflammatory markers in the CNS tissues, the responses of SHBRV-17-infected mice were equal to or greater than those of CVS-F3-infected coun-

terparts in the cerebellum, the primary location of the enhanced BBB permeability and CNS inflammation associated with the clearance of CVS-F3 (21). Consistent with the upregulation of TNF-α and ICAM-1 mRNAs, enhanced ICAM-1 expression can be readily visualized on the neurovasculature of the cerebellum in both CVS-F3- and SHBRV-17-infected mice. This suggests that any activated RV antigen-specific lymphocytes present in the circulation should be capable of adhering to neurovascular endothelial cells.

If the proinflammatory response in the CNS of SHBRV-17-infected mice is intact, the inability of immune cells to infiltrate the cerebellum is more likely to result from a deficit in the mechanism that allows these cells to cross the BBB. Conceivably, this could be at the level of either immune cell or BBB function. We did not detect any reduction in the development of an RV antigen-specific humoral response between SHBRV-17- and CVS-F3-infected mice. Moreover, as has previously been demonstrated for the clearance of CVS-F3 from the CNS, the isotype of the RV-specific antibodies produced by SHBRV-17-infected mice is IgG2a. This indicates a bias toward the Th1 cell reactivity that predominates in other CNS inflammatory reactions (7, 22, 23). The argument that the cells of the adaptive immune response are fully functional in SHBRV-17-infected mice is supported by the observation that lymphocytes from SHBRV-17-infected mice are capable of enhancing BBB permeability, invading CNS tissues, and clearing CVS-F3 when adoptively transferred into infected $rag$-$2^{-/-}$ mice.

Although CVS-F3 can be cleared from the CNS by RV-specific lymphocytes raised in either CVS-F3- or SHBRV-17-infected mice, neither effector cell population can clear SHBRV-17 from CNS tissues. The transfer of lymphocytes from SHBRV-17- and CVS-F3-infected mice can protect naive recipients against subsequent infection with SHBRV-17, presumably by preventing the spread of the virus to the CNS. However, we have found that neither cell population can prevent lethal rabies when SHBRV-17 infection precedes adoptive transfer by as little as several hours. In these experiments, antiviral immunity was allowed to develop for 6 days in the donor animals and transferred cells had an additional 7 to 8 days to mediate a protective response before the recipients died. Considering that clearance of CVS-F3 begins approximately 6 days after infection, this should have been sufficient time to mediate a protective response against SHBRV-17. The fact that the course of the disease was unchanged suggests that the adoptively transferred cells had no impact on the replication and spread of the virus in the CNS.

We speculate that the inability to "open" the BBB in the cerebellum and deliver the appropriate immune effectors to the CNS tissues is the fundamental deficit that prevents immune clearance of SHBRV-17 from the CNS and ultimately leads to the death of infected animals. While CD8 T cells are important in clearing some viruses from the CNS, the primary effectors of RV clearance are VNAs (10, 13) that must either cross the BBB or be produced in the CNS tissues by invading B cells. In our studies of CVS-F3 clearance from CNS tissues, enhanced BBB permeability was associated with invasion of the CNS by CD4 T cells and B cells but not with CD8 T-cell accumulation (21). Correlations between the patterns of BBB permeability changes and the appearance of CD4 and IFN-γ

mRNAs in CNS tissues have led us to speculate that the enhanced BBB permeability associated with the delivery of B cells and antibody to the CNS of CVS-F3-infected mice is driven by CD4 T cells through an IFN-γ-dependent process (21). The failure of this mechanism could be why conventional postexposure treatment of rabies is ineffective once the virus has reached CNS tissues and clinical signs of the disease have developed (3, 27). We suggest that at some time after the virus has reached the CNS tissues, the BBB in the cerebellum becomes refractory to the signals that trigger enhanced permeability. Consequently, immune effectors cannot reach the CNS tissues to clear the virus. This is consistent with observations made in clinical rabies that people who die from rabies in the absence of treatment often develop RV-specific antibodies (15). The idea that the development of enhanced BBB permeability is a critical checkpoint in the response to RV infection of the CNS is also supported by a recent human rabies case where an individual who did not receive PEP recovered despite developing advanced clinical signs of infection (5). In this case, the victim naturally developed a high VNA titer and enhanced BBB permeability as evidenced by the appearance of serum proteins in the cerebrospinal fluid (26). Even in the absence of PEP, the indigenous immune response to RV in this individual was sufficient to clear the infection from the CNS. Since RV can be cleared from the CNS if immune effectors have access to the infected tissues, we believe that the development of an approach to circumvent the maintenance of BBB integrity in RV-infected individuals may have therapeutic value.

The existence of a mechanism to maintain BBB integrity and prevent the delivery of immune effectors to CNS tissues has implications for a variety of CNS diseases. It is conceivable that this mechanism interferes with the clearance of other neurotropic virus and possibly with CNS tumor immunity. From the opposite perspective, the ability to trigger such a mechanism may have therapeutic value for neurodegenerative diseases associated with a reduction of BBB integrity.

## REFERENCES

1. **Centers for Disease Control and Prevention.** 1991. Epidemiologic notes and reports human rabies—Texas, Arkansas, and Georgia, 1991. Morb. Mortal. Wkly. Rep. **40:**765–769.
2. **Centers for Disease Control and Prevention.** 1993. Human rabies—New York, 1993. Morb. Mortal. Wkly. Rep. **42:**799, 805–806.
3. **Centers for Disease Control and Prevention.** 1999. Human rabies prevention—United States, 1999. Recommendations of the Advisory Committee on Immunization Practice. Morb. Mortal. Wkly. Rep. **48:**1–21.
4. **Centers for Disease Control and Prevention.** 1994. Human rabies—Texas and California, 1993. Morb. Mortal. Wkly. Rep. **43:**93–96.
5. **Centers for Disease Control and Prevention.** 2004. Recovery of a patient from clinical rabies—Wisconsin, 2004. Morb. Mortal. Wkly. Rep. **53:**1171–1173.
6. **Champion, J. M., R. B. Kean, C. E. Rupprecht, A. L. Notkins, H. Koprowski, B. Dietzschold, and D. C. Hooper.** 2000. The development of monoclonal human rabies virus neutralizing antibodies as a substitute for pooled human immune globulin in the prophylactic treatment of rabies virus exposure. J. Immunol. Methods **235:**81–90.
7. **Chang, J. R., E. Zaczynska, C. D. Katsetos, C. D. Platsoucas, and E. L. Oleszak.** 2000. Differential expression of TGF-β, IL-2, and other cytokines in the CNS of Theiler's murine encephalomyelitis virus-infected susceptible and resistant strains of mice. Virology **278:**346–360.
8. **Dietrich, J. B.** 2002. The adhesion molecule ICAM-1 and its regulation in relation with the blood-brain barrier. J. Neuroimmunol. **128:**58–68.

9. **Dietzschold, B., K. Morimoto, D. C. Hooper, J. S. Smith, C. E. Rupprecht, and H. Koprowski.** 2000. Genotypic and phenotypic diversity of rabies virus variants involved in human rabies: implications for postexposure prophylaxis. J. Hum. Virol. **3:**50–57.

10. **Dietzschold, B., M. Kao, Y. M. Zheng, Z. Y. Chen, G. Maul, Z. F. Fu, C. E. Rupprecht, and H. Koprowski.** 1992. Delineation of putative mechanisms involved in antibody-mediated clearance of rabies virus from the central nervous system. Proc. Natl. Acad. Sci. USA **89:**7252–7256.

11. **Dietzschold, B., W. H. Wunner, T. J. Wiktor, A. D. Lopes, M. Lafon, C. Smith, and H. Koprowski.** 1983. Characterization of an antigenic determinant of the glycoprotein which correlates with pathogenicity of rabies virus. Proc. Natl. Acad. Sci. USA **80:**70–74.

12. **Hooper, D. C.** 2002. Rabies virus, p. 742–748. *In* N. R. Rose, R. G. Hamilton, and B. Detrick (ed.), Manual of clinical laboratory immunology, 6th ed. ASM Press, Washington, D.C.

13. **Hooper, D. C., K. Morimoto, M. Bette, E. Weihe, H. Koprowski, and B. Dietzschold.** 1998. Collaboration of antibody and inflammation in clearance of rabies virus from the central nervous system. J. Virol. **72:**3711–3719.

14. **Hughes, G. J., J. S. Smith, C. A. Hanlon, and C. E. Rupprecht.** 2004. Evaluation of a TaqMan PCR assay to detect rabies virus RNA: influence of sequence variation and application to quantification of viral loads. J. Clin. Microbiol. **42:**299–306.

15. **Kasempimolporn, S., T. Hemachudha, P. Khawplod, and S. Manatsathit.** 1991. Human immune response to rabies nucleocapsid and glycoprotein antigens. Clin. Exp. Immunol. **84:**195–199.

16. **Kean, R. B., S. Spitsin, T. Mikheeva, G. Scott, and D. C. Hooper.** 2000. The peroxynitrite scavenger uric acid prevents inflammatory cell invasion into the CNS in experimental allergic encephalomyelitis through maintenance of blood-CNS barrier integrity. J. Immunol. **165:**6511–6518.

17. **Kissi, B., N. Tordo, and H. Bourhy.** 1995. Genetic polymorphism in the rabies virus nucleoprotein gene. Virology **209:**526–537.

18. **Messenger, S. L., J. S. Smith, L. A. Orciari, P. A. Yager, and C. E. Rupprecht.** 2003. Emerging pattern of rabies deaths and increased viral infectivity. Emerg. Infect. Dis. **9:**151–154.

19. **Miyamoto, K., and S. Matsumoto.** 1967. Comparative studies between pathogenesis of street and fixed rabies infection. J. Exp. Med. **125:**447–456.

20. **Murphy, F. A.** 1977. Rabies pathogenesis. Arch. Virol. **54:**279–297.

21. **Phares, T. W., R. B. Kean, T. Mikheeva, and D. C. Hooper.** 2006. Regional differences in blood-brain barrier permeability changes and inflammation in the apathogenic clearance of virus from the central nervous system. J. Immunol. **176:**7666–7675.

22. **Shankar, V., M. Kao, A. N. Hamir, H. Sheng, H. Koprowski, and B. Dietzschold.** 1992. Kinetics of virus spread and changes in levels of several cytokine mRNAs in the brain after intranasal infection of rats with Borna disease virus. J. Virol. **66:**992–998.

23. **Silver, N., C. Good, M. Sormani, D. MacManus, A. Thompson, M. Filippi, and D. Miller.** 2001. A modified protocol to improve the detection of enhancing brain and spinal cord lesions in multiple sclerosis. J. Neurol. **248:**215–224.

24. **Wang, Z. W., L. Sarmento, Y. Wang, X. Li, V. Dhingra, T. Tseggai, B. Jiang, and Z. F. Fu.** 2005. Attenuated rabies virus activates, while pathogenic rabies virus evades, the host innate immune responses in the central nervous system. J. Virol. **79:**12554–12565.

25. **Wiktor, T. J., P. C. Doherty, and H. Koprowski.** 1977. Suppression of cell-mediated immunity by street rabies virus. J. Exp. Med. **145:**1617–1622.

26. **Willoughby, R. E., K. S. Tieves, G. M. Hoffman, N. S. Ghanayem, C. M. Amelie-Lefond, M. J. Schwabe, M. J. Chusid, and C. E. Rupprecht.** 2005. Brief report: survival after treatment of rabies with induction of coma. N. Engl. J. Med. **352:**2508–2514.

27. **World Health Organization Expert Committee on Rabies.** 1992. 8th report. WHO Tech. Rep. Ser. **824:**1–84.

28. **Yan, X., M. Prosniak, M. T. Curtis, M. L. Weiss, M. Faber, B. Dietzschold, and Z. F. Fu.** 2001. Silver-haired bat rabies virus variant does not induce apoptosis in the brain of experimentally infected mice. J. Neurovirol. **7:**518–527.